



Kinetics and morphology analysis of struvite precipitated from aqueous solution under the influence of heavy metals: Cu^{2+} , Pb^{2+} , Zn^{2+}



D.S. Perwitasari^a, S. Muryanto^b, J. Jamari^c, A.P. Bayuseno^{c,*}

^a Department of Chemical Engineering, Universitas Pembangunan Nasional "Veteran" Jawa Timur, Surabaya, East Java, Indonesia

^b Department of Chemical Engineering, UNTAG University in Semarang, Bendhan Dhuwur Campus, Semarang 50233, Indonesia

^c Department of Mechanical Engineering, Diponegoro University, Tembalang Campus, Semarang 50275, Indonesia

ARTICLE INFO

Keywords:

Struvite
Heavy metals
Kinetics
XRPD Rietveld
Morphology

ABSTRACT

The present study examined the influence of metal ions (Cu^{2+} , Pb^{2+} , and Zn^{2+}) on kinetics and morphology of struvite precipitated from aqueous solutions containing equimolar ratios of struvite components: Mg^{2+} , NH_4^+ , PO_4^{3-} . Kinetics of the struvite precipitation in the presence of metal ions [0, 1, 10, 50 and 100 ppm] was evaluated through the change of pH of the precipitating solution. The kinetic evaluation demonstrated that the precipitation satisfactorily followed the first-order kinetic with respect to Mg^{2+} . It was found that for the three metal ions tested, the higher the concentrations of the metal ions: 0, 1, 10, 50, 100 ppm, the less the crystals obtained and the lower the rate constants. Depending on the concentrations of the metal ions added into the solution, the rate constants varied from 4.344 to 1.056 h^{-1} which agree with most published values. It was postulated that the metal ions were adsorbed onto the surface of the crystals and hence retarded the growth. The crystals obtained were characterized using SEM-EDX and XRPD Rietveld. The characterization revealed that the precipitates were mainly struvite of various sizes (between 10 and 60 μm) with sylvite as impurities. It is envisaged that the present study would add to the understanding of the removal of metal ions from industrial wastewater through struvite precipitation.

1. Introduction

Wastewater contains a particularly high concentration of phosphate, potassium, and ammonia which may cause eutrophication of surface waters [1]. The phosphorus concentrations in the wastewater can be reduced through mass crystallization of sparing struvite [$\text{MgNH}_4\text{PO}_4 \cdot 6\text{H}_2\text{O}$] on a mechanical mixing equipment [2,3]. In addition, the wastewater containing heavy metals namely, copper (Cu^{2+}), lead (Pb^{2+}) and zinc (Zn^{2+}), could have a negative effect on health, environment, equipment, and the aesthetic quality of the water bodies. Correspondingly, traces of heavy metals contaminated wastewater must be treated prior to its release to the environment [4,5].

Toxic heavy metals from inorganic effluent can be stabilized through conventional methods such as precipitation, cementation, sedimentation, filtration, coagulation, flotation, ion exchange and, adsorption [6–8]. However, these methods often lead to incomplete treatment, high-energy consumptions, and still produce an output of toxic sludge or waste products [9]. In this way, the conventional precipitation of heavy metals to yield hydroxides have shown the ineffectiveness in metal immobilization, especially when their

concentrations are low in the solution. Alternatively, heavy metals in the wastewater can be removed simultaneously from the wastewater with a recovery of potassium, phosphate and ammonia using the precipitation agents [e.g., KOH and $\text{Mg}(\text{OH})_2$], to produce struvite and/or struvite-K [$\text{KMgPO}_4 \cdot 6\text{H}_2\text{O}$ -(KMP)] [10]. Currently, the recovery of six heavy metals [Cu, Ni, Pb, Zn, Mn, Cr (III)] from solutions can be enhanced by utilizing the self-synthesized struvite under pH variations of 6.0–10.0. Results indicated that more than 95% of those six heavy metals could be taken out from the solution by struvite precipitation [11], and the precipitating solid contains the highest quality of struvite (97%) which could be potentially utilized as fertilizer [12].

Correspondingly, several kinds of reactor systems have been developed to facilitate the wastewater treatment for not only sustainable recovery of phosphorus but also the adsorption of metals and organics into the surface of crystal struvite [5]. Consequently, the heterogeneous nucleation mechanism and crystal growth of struvite may be influenced by the presence of heavy metals. The exchange between ionized metals such as cadmium, zinc, and nickel with magnesium can occur in the crystal lattice of struvite [3]. Therefore, the interaction between metals and struvite during co-precipitation and adsorption have become a

* Corresponding author.

E-mail addresses: sariyah05@gmail.com (D.S. Perwitasari), apbayuseno@gmail.com (A.P. Bayuseno).

great concern. Knowledge of the heterogeneous nucleation in terms of the speed of nucleation and the crystal growth has received much attention for reducing the activation energy due to the catalytic effect of metal ion particles [2]. The presence of heavy metals may deteriorate the morphology of the precipitates and, in certain cases, cause the precipitation of a less stable phase instead of struvite. The advancement from the previous study [13] is shown by the findings on rate constants for the three metal ions investigated. In addition, the present study compared characterization of the precipitates with predicted precipitation using Visual Minteq. Industrialization and urbanization cause a serious problem for the environment and especially the life forms due to excessive release of heavy metals into water sources. Heavy metal ions are known to be non biodegradable and may accumulate in living tissues. Among these eco-toxic metal ions are Pb^{2+} , Cu^{2+} , and Zn^{2+} . Many industrial activities for the manufacture of batteries, ammunition, various metal products and ceramic discharge Pb^{2+} into the water bodies [14]. Copper is used extensively in various industries including refineries, paper and pulp, fertilizer, mining, and electroplating [15]. Meanwhile, industrial effluents from pulp and paper mills, organic and inorganic chemical plants, petroleum and petrochemicals, steel work foundries, and steam generation power plants may contain Zn^{2+} [16].

Microstructure and property evaluation results of selected heavy metals incorporated into the crystal lattice of struvite are required to control the quality of recovered products. The characterization methods are needed here to examine the struvite quality flushing out of the reactors. Mineralogy, morphology and final particle size are the key factors in assuring for phosphorus recovery efficiency [2].

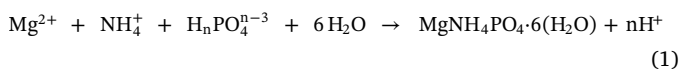
So far there is no report on the influence of three metal ions, Pb^{2+} , Cu^{2+} , and Zn^{2+} , on struvite precipitation. Therefore, the objectives of this study were to examine the struvite precipitation under the individual influence of these metals from a kinetic and morphological point of view. This study could be useful for determining the struvite precipitation as a means of fouling prevention and mitigation in which the effluent contains heavy metal ions.

2. Materials and methods

2.1. Analytical methods and kinetic study of struvite precipitation

The crystal synthesis was performed by chemical precipitation from a synthetic waste solution, of which a mixture of 0.25 M MgCl_2 and 0.25 M $[(\text{NH}_4)_2\text{H}_2\text{PO}_4]$ solutions were prepared, and all chemicals were analytically pure grade (Merck™). In the real wastewater condition, a low magnesium content relative to ammonia and phosphates is commonly found and magnesium is added to promote the struvite crystallization process. For magnesium source, MgCl_2 was particularly added in the solution due to its high solubility [17].

Solutions of MgCl_2 and $[(\text{NH}_4)_2\text{H}_2\text{PO}_4]$ were filtered through 0.45 mm paper filter and reserved at least 24 h just prior to conducting experiments. The series of struvite precipitation experiments were carried out in a clean glass beaker of one-liter volume stirred at 200 rpm and equipped with temperature control unit. Adjusting pH to an initial value of 6.5 was performed by dropping wisely an aqueous solution of 0.5 M KOH during mixing of MgCl_2 and $[(\text{NH}_4)_2\text{H}_2\text{PO}_4]$ solutions, of which the molar ratio of Mg^{2+} : NH_4^+ : PO_4^{3-} (MAP) was determined as 1:1:1. The struvite precipitation can be expressed as the Eq. (1) (with $n = 0, 1, \text{ and } 2$) [18].



The concentration of $[\text{Mg}^{2+}]$ changed over time and the kinetic constants of struvite crystals were estimated according to the following Eq. (2) [13].

$$\ln(C - C_{\text{eq}}) = -k t + \ln(C - C_0) \quad (2)$$

Table 1
Chemical compositions of the synthetic wastewater used in the study.

Ions	PO_4^{3-}	NH_4^+	Mg^{2+}	K^+	Cl^-
(mol/kg)	0.14590	0.27290	0.16190	0.16890	0.07710

where $C = [\text{Mg}^{2+}]$ at any time t (molar)

$C_{\text{eq}} = [\text{Mg}^{2+}]$ at equilibrium (molar)

$C_0 =$ initial $[\text{Mg}^{2+}]$ at time zero ($t = 0$) (molar)

$k =$ reaction rate constant (h^{-1})

$t =$ crystallization time (min)

Furthermore, the reactions were conducted in duplicate for kinetic data. All precipitation experiments were performed at room temperature (30°C). To control the temperature of the solution used a thermostatic controller during the kinetic experiments. Solution pH was continuously monitored using an Orion SA520 pH meter with a gel epoxy probe. The obtained precipitate was then filtered off in a paper (Schleicher&Schuell no. 604), washed with distilled water, and dried directly on the filter at room temperature. The entire time of the precipitation and filtration of struvite required 90 min. The mass scale was then measured by weighing the dried sample.

The effects of Cu^{2+} , Pb^{2+} and Zn^{2+} ions (0, 1, 10, 50 and 100 ppm) on struvite precipitation were evaluated in this work. In this experiment, each crystal of CuCl_2 , PbCl_2 , and ZnCl_2 was diluted into 500 ml volume of MgCl_2 solution. The ions concentration present in the synthetic solution including K^+ from KOH addition is presented in Table 1.

2.2. Chemical thermodynamic modeling

The struvite precipitation potential in the synthetic wastewater was examined using a thermodynamic chemical equilibrium model developed with the Visual Minteq software program version 3.0 [19]. Calculations were conducted using the Davies activity coefficient approximation. The program was employed to calculate the solution equilibrium model using the input data of ion concentrations in the synthetic wastewater. The Visual Minteq was selected in the study to predict the mineral speciation formed in the solution. The chemical composition of the synthetic wastewater for the input of the program is given in Table 1. The model of mineral species was subsequently calculated by the program, using pH values and temperatures of 30°C as an input parameter. The mineral species predicted by the program were subsequently justified by the X-ray powder diffraction (XRPD) Rietveld method [20].

2.3. Materials characterization

The dried samples of precipitates were characterized through SEM coupled with an energy dispersive X-ray analysis (SEM-EDX) and XRPD method. The precipitates were ground with a pestle and mortar to obtain a powder with sizes $< 75 \mu\text{m}$. Samples with different particle sizes were embedded in epoxy on a glass slide and then sputtered with gold for SEM analysis.

Instead, the ground powder was placed in an aluminum sample holder for XRPD measurement by A Philips PW 1710 Diffractometer equipped with a Cu tube. The measured XRPD data are shown in Table 2. Identification of crystalline phases was initially performed with (Powder Diffraction File) – PDF-2 Phillips software. The candidate crystalline phases found by the search match method were then verified by the Rietveld refinement method with Program Fullprof-2k, version 3.30 [21]. The crystal structure model for the Rietveld method was obtained from the literature [AMCSD-American mineralogist of crystal structure database]. The full-width at half-maximum (FWHM) of XRPD peak profiles as a function of $\tan(\theta)$ was fitted by the Fullprof program using the u-v-w formula of Caglioti et al. [22]. The cell parameters were received from the refinement, which then was used for determination of

Table 2
The XRPD data measured for the Rietveld refinement.

Geometry	Bragg-Brentano
Goniometer radius	240 mm
Radius source	CuK α
Generator	40 kV, 30 mA
Tube	Normal focus 10 × 1 mm
Divergence and receiving slits	0.2117°
Soller slits	5.3°
Resolving slit	100 mm
Monochromator	Graphite (diffracted beam)
Detector	Scintillation counter
The scan parameters and step size	5–90° 2 θ in 0.020° increments
Integration time	10 s

the weight.% levels of mineralogical phases. Calculation procedures of the refinement are provided elsewhere [23].

3. Results and discussion

3.1. Effect of pH on metal adsorption in struvite crystal

The time profiles of pH in the solution in the presence of different concentrations of Cu²⁺ are shown in Fig. 1a. In the absence of Cu²⁺, a rapid reduction of the pH was observed during the first 10 min corresponding to the removal of magnesium from solution. The pH reduction was caused by struvite precipitation. From about 60 to 90 min toward the end of the experiment, the pH level for the three metal ions tested was almost constant, indicating the completion of the precipitation. With increasing concentration of Cu²⁺ (1–100 ppm), the pH decreases gradually until stabilized because the crystallization process of struvite is inhibited by the addition of metal ions concentration. Similar trends were also observed in the time pH profile in the absence and presence of Pb²⁺ and Zn²⁺ (1–100 ppm) in the aqueous solution (Fig. 1b and c). It was postulated that the metal ions were adsorbed onto the surface of the crystals and hence retarded the growth. Accordingly, the removal efficiency of the metal ions could be lower. Here initial pH plays an important role for adsorption of the metal ions. The significant removal efficiency of heavy metals was reported at pH 1.0–4.0 but the efficiency is improved slightly with pH > 4.0 [7]. In this way, ion exchange between Mg²⁺ and the heavy metal ions may occur in struvite surface.

3.2. Adsorption kinetics of metals

Struvite crystallization can be well represented by Eq. (1) [24]. Hence, kinetics of the struvite precipitation was evaluated through the change of pH of the precipitating solution. The kinetic evaluation demonstrated that the precipitation satisfactorily followed the first-order kinetic with respect to Mg²⁺ as reported in Eq. (2). It is known, the rate constant, could have a substantial negative correlation between the quantities of metal ions dissolved in the solution [13]. Therefore, the adsorption kinetics of metal ions onto struvite surface were examined by the kinetic model of the first-order of Eq. (2). Fig. 2a shows the line of best fit for the typical experimental run of initial 10 min in the absence of metal ions. The struvite crystallization is well exemplified by the first-order kinetics model with a high correlation coefficient (R²) of 0.9775 (Fig. 2a-left). During 10–70 min, the reaction followed the first order rate kinetic model with R² of 0.9549 (Fig. 2a-right). Hence, two forms of the kinetic may follow the crystallization of struvite. Kinetic adsorption data (0–60 min) in the presence of 1 ppm metal ions could be fitted to Eq. (2) with the best correlation coefficients (Fig. 2b). The adsorption rate constant of Cu²⁺ was calculated from the slopes of the straight lines, and the values were presented in Table 3. The experimental runs at 30 °C and in the absence of metals yields the lines corresponding to the first order rate equation, of which the calculated rate value of 4.334 h⁻¹ is in close agreement with results presented in the

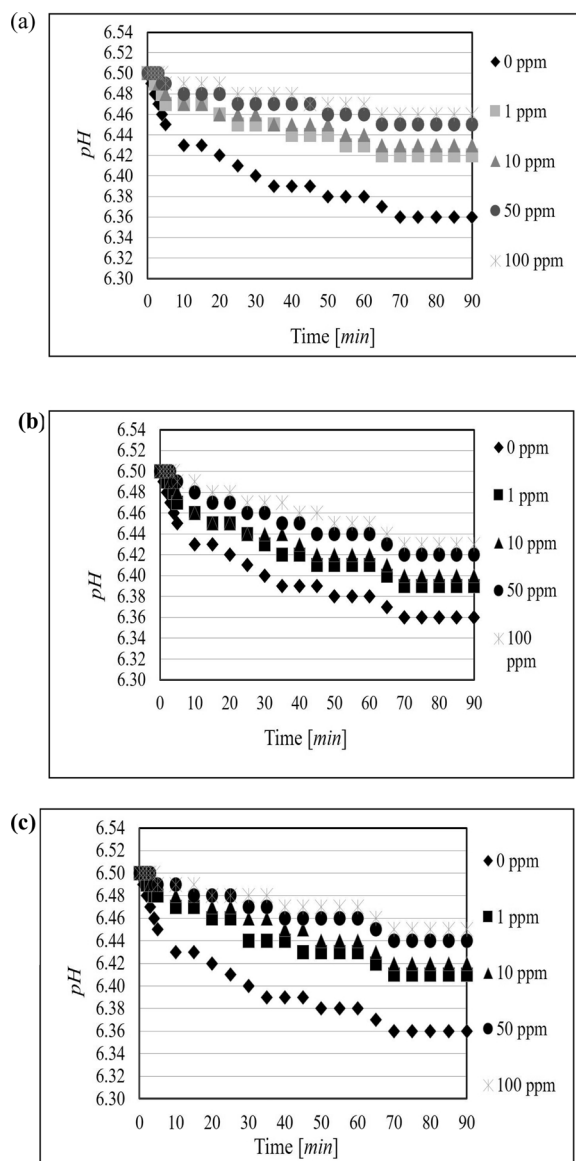


Fig. 1. Variation of pH in the presence of a) Cu²⁺; b) Pb²⁺ and c) Zn²⁺ in the solution.

literature [25–27]. Moreover, the rate constant of Cu²⁺ (1–100 ppm) present in the solution was all lower than that in the absence of Cu²⁺.

Further, the adsorption rate constants of Pb²⁺ and Zn²⁺ (1–100 ppm) were similarly calculated from the slopes of the straight lines, and the values were listed in Tables 4 and 5. Obviously, the rates of the three metal ions tested decreased with increasing concentrations from 1 to 100 ppm. Moreover, the percentage of inhibition for struvite precipitation could be estimated from the calculation between the highest rates (0 ppm) and the lowest rates (100 ppm) of Cu²⁺, Pb²⁺ and Zn²⁺ as follows: [(4.344–1.512)/4.344] × 100% = 65.19%; [(4.344–1.338)/4.344] = 69.42%; [(4.344–1.056)/4.344 = 75.6%], respectively. The maximum inhibition of growth rate was found for Zn²⁺. This adsorption may be controlled by a physical adsorption process [8]. It is assumed, the ions could be adsorbed onto the surface during developing crystal nuclei and thus prohibiting their outgrowth beyond the critical size for further growth [28]. This effect could be seen in the result of mass scale precipitated in the solution due to the presence of Zn²⁺ (Table 5).

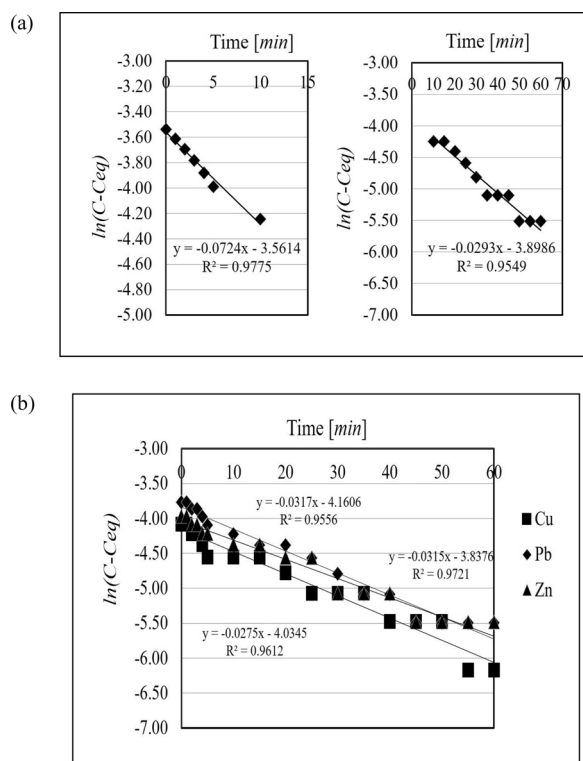


Fig. 2. Curve fitting of the calculated $[Mg^{2+}]$ for the first-order kinetic; a) in the absence of metals ions b) in the presence of 1 ppm metal ions Cu^{2+} , Pb^{2+} , Zn^{2+} .

Table 3

Mass scale and the rate constants for struvite crystallization in the presence of Cu^{2+} .

Cu^{2+} (ppm)	Mass (mg)	Regression equation	Rate constant (h^{-1})	R^2
0	11.474	$y = -0.0724x - 3.5614$	4.344	0.9775
1	10.906	$y = -0.0317x - 4.1606$	1.902	0.9556
10	9.849	$y = -0.0302x - 4.2870$	1.812	0.9488
50	9.117	$y = -0.0267x - 4.5936$	1.602	0.9331
100	8.341	$y = -0.0252x - 4.7374$	1.512	0.9320

Note: Initial period of 0–10 min for calculating rate in the absence metal ions; 0–60 min for the rates in the presence of metal ions.

Table 4

Mass scale and the rate constants for struvite crystallization in the presence of Pb^{2+} .

Pb^{2+} (ppm)	Mass (mg)	Regression equation	Rate constant (h^{-1})	R^2
0	11.474	$y = -0.0724x - 3.5614$	4.344	0.9775
1	11.033	$y = -0.0315x - 3.8376$	1.890	0.9721
10	10.828	$y = -0.0294x - 3.9267$	1.764	0.9589
50	9.469	$y = -0.0262x - 4.0822$	1.572	0.9740
100	8.992	$y = -0.0223x - 4.1714$	1.338	0.9687

Note: Initial period of 0–10 min for calculating rate in the absence metal ions; 0–60 min for the rates in the presence of metal ions.

Table 5

Mass scale and the rate constants for struvite crystallization in the presence of Zn^{2+} .

Zn^{2+} (ppm)	Mass (mg)	Regression equation	Rate constant (h^{-1})	R^2
0	11.474	$y = -0.0724x - 3.5614$	4.344	0.9775
1	11.324	$y = -0.0275x - 4.0345$	1.650	0.9612
10	10.965	$y = -0.0242x - 4.0716$	1.452	0.9743
50	9.848	$y = -0.0211x - 4.3836$	1.266	0.9469
100	9.141	$y = -0.0176x - 4.5671$	1.056	0.9322

Note: Initial period of 0–10 min for calculating rate in the absence metal ions; 0–60 min for the rates in the presence of metal ions.

3.3. Chemical equilibrium model of mineral precipitation

The possible precipitation of minerals in the solution containing metal ions was examined at $pH = 6.5$ using the software Visual Minteq. In this way, the solid mineral precipitation corresponds to the level of supersaturation in the solution, which is represented as a saturation index (SI) as follows: $SI = \log [IAP/Ksp]$, where IAP is the ion activity product of species, and Ksp is the solubility product of mineral. Here, SI can be utilized to predict the saturation state of the precipitating mineral. Under supersaturated solution ($SI > 0$), a spontaneous precipitation occurs, while the result is considered equilibrium when $SI = 0$. Moreover the under saturated solution ($SI < 0$), no possible precipitation take place. In the present study, SI was calculated for the various solid phases and the results are given in Table 6.

Saturation index in the solution, according to the above calculation, suggested the possibility of other precipitation products over struvite. Indeed, the presence of Mg^{2+} and PO_4^{-3} can determine the formation of $Mg_3(PO_4)_2$ ($SI = 0.971$) or $MgHPO_4 \cdot 3H_2O$ ($SI = 0.992$), besides the struvite ($SI = 1.359$) formation. The simulations were then done by varying the Cu^{2+} , Pb^{2+} and Zn^{2+} contents and maintaining the MAP ratio equal to 1: 1: 1. As expected, struvite (K) formation did not occur [$SI = -0.861$]. Conversely, the other possible metal (M^{+}) compounds [such as $Cu(OH)_2$, $Cu_3(PO_4)_2 \cdot 3H_2O$, chloropyromorphite [$Pb_5(PO_4)_3Cl$], hydroxylpyromorphite [$Pb_5(PO_4)_3OH$], $Zn_5(OH)_8Cl_2$, $Zn_3(PO_4)_2 \cdot 4H_2O$] may precipitate on the solution due to its greater SI level. It was reported that 100% MAP formation occurred by struvite when MAP ratio was equal to 1:1:1. Struvite (K) presence was null at various concentrations of metal ions/. Therefore, this mineral formation was predicted to be absent in the precipitate.

3.4. Surface characterization of the precipitates

Surface characterization of the precipitates was employed to justify the predicted minerals by Visual Minteq. Fig. 3a illustrates the results of XRPD analysis, which indicated that the prominent characteristic peaks of precipitate were close to those of struvite pattern standard [PDF#71-2089] in addition to sylvite (KCl) [PDF# 76-3368]. The results of the XRPD Rietveld analysis also proved that the XRPD intensity of the solid conformed to that of the struvite and sylvite patterns as shown in Fig. 3b. The XRPD Rietveld program confirmed struvite to be crystalline in the orthorhombic system (space group $Pm2_1n$) with the lattice parameters $a = 6.9335 \text{ \AA}$, $b = 6.1422 \text{ \AA}$ and $c = 11.1784 \text{ \AA}$ [29]. Additionally, the KCl peaks were identified at the precipitate [30], which could be attributed to the crystallization of excessive potassium reacted with chloride ion in the solution. The recovered precipitates were filtered and then washed lightly with distilled water, followed by air drying. It was assumed that only chlorides and alkali ions were removed from the surface of the precipitates during washing, leaving the struvite crystals mass unaffected. The mass of sylvite in the recovered

Table 6

The predicted mineral speciation of the precipitating solid.

The presence of Cu^{2+}		The presence of Pb^{2+}		The presence of Zn^{2+}	
Mineral	SI	Mineral	SI	Mineral	SI
$\text{Cu}_2\text{Cl}(\text{OH})_3$	8.761	Chloropyromorphite	49.578	$\text{Mg}_3(\text{PO}_4)_2$	0.519
$\text{Cu}(\text{OH})_2$	2.734	Cotunnite (PbCl_2)	0.063	$\text{MgHPO}_4 \cdot 3\text{H}_2\text{O}$	0.74
$\text{Cu}_3(\text{PO}_4)_2$	13.982	Hydroxypyromorphite	36.073	KCl	-3.493
$\text{Cu}_3(\text{PO}_4)_2 \cdot 3\text{H}_2\text{O}$	12.252	Laurionite	2.871	Struvite	1.565
KCl	-3.058	KCl	-3.339	Struvite (K)	-1.107
$\text{Mg}_3(\text{PO}_4)_2$	0.971	$\text{Mg}_3(\text{PO}_4)_2$	2.427	Zincite	2.029
$\text{MgHPO}_4 \cdot 3\text{H}_2\text{O}$	0.992	$\text{MgHPO}_4 \cdot 3\text{H}_2\text{O}$	1.795	$\text{Zn}(\text{OH})_2$	0.773
Periclase	-9.09	$\text{Pb}(\text{OH})_2$	3.648	$\text{Zn}_2(\text{OH})_3\text{Cl}$	2.508
Struvite	1.359	$\text{Pb}_2(\text{OH})_3\text{Cl}$	6.33	$\text{Zn}_3(\text{PO}_4)_2 \cdot 4\text{H}_2\text{O}$	15.332
Struvite (K)	-0.861	Struvite	2.799	$\text{Zn}_5(\text{OH})_8\text{Cl}_2$	9.898
Tenorite (CuO)	3.568	Struvite (K)	-0.064	ZnCl_2	-10.443

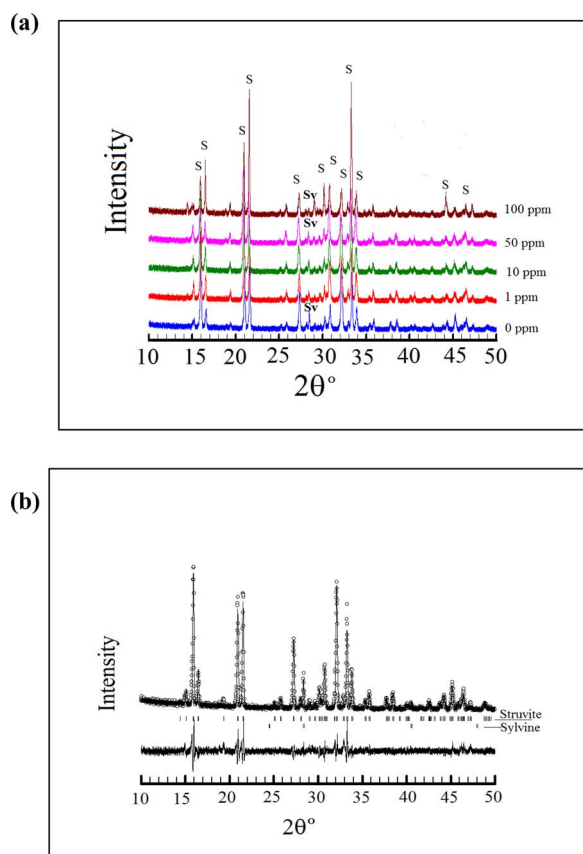


Fig. 3. a) XRPD patterns of precipitate in the presence of various concentrations (0–100 ppm) of Cu^{2+} ; b) Plot of XRPD Rietveld analysis of the crystals precipitated in the absence of Cu^{2+} . The peaks are labelled S (struvite) and Sv (sylvite).

products was assumed to be negligible. This washing procedure was the same as reported in our previous studies [31,23]. Conversely, the metal bearing minerals could not be detected by XRPD, this could explain that the metal content is under x-ray detection limit (< 0.3 wt.%). Indeed, increasing concentrations of Cu^{2+} did not change phase compositions of the precipitate, of which struvite is a still dominant mineral. Likewise, the addition of various concentrations of Pb^{2+} and Zn^{2+} did not alter the mineral compositions of the precipitate (Fig. 4).

The formation of struvite was also confirmed by SEM/EDX analysis. A prismatic shaped like morphology developed in the solution without the effect of Cu^{2+} is a typical synthetic struvite (Fig. 5a) [29,31], and its size was irregular (10–60 μm). The EDX spectrum for struvite precipitated with the addition of one of the metal ions (Cu^{2+}). (Fig. 5b) shows traces of Cu^{2+} . This demonstrates that Cu^{2+} could either have

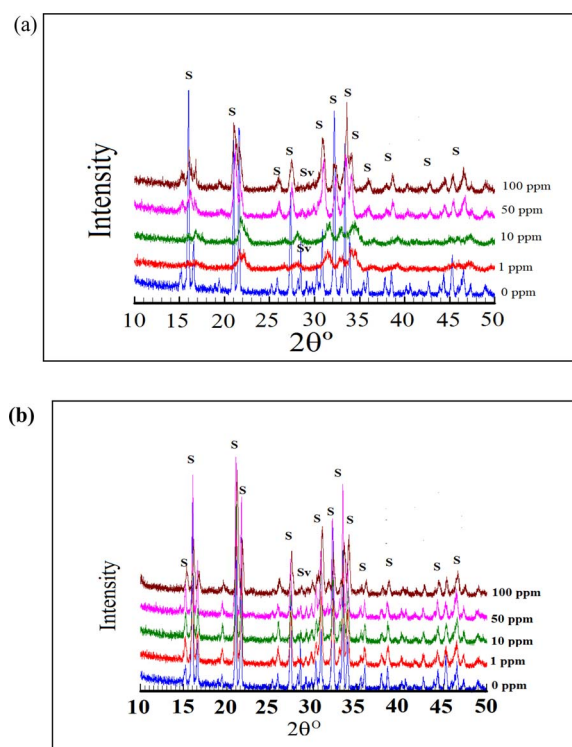


Fig. 4. XRPD patterns of precipitate in the presence of various concentrations (0–100 ppm) of: a) Pb^{2+} and b) Zn^{2+} . The peaks are labelled S (struvite) and Sv (sylvite).

been adsorbed onto the surface of the crystals or embedded into the crystal lattice. Similar cations of Pb^{2+} and Zn^{2+} could be also adsorbed in the struvite structure, as revealed by EDX (Fig. 6a and b), leading to dramatically distort the shape of crystals. Apparently struvite crystal growth was suppressed by the presence of metal ions even in trace amounts from 0.00 to 100 ppm, as indicated in the crystal size reduction.

The results of the XRPD semi-quantitative analysis, summarized in Table 7, show that all samples are mainly composed by struvite which explains the MAP ions to be recovered by the precipitation method. Sylvite could be also found in smaller quantities (0.2–1.5 wt.%). According to the SEM-EDX observations of samples (Figs. 5 and 6), struvite (primary phosphate) could be associated with metal ions present in the solution. In a general way, SEM observations showed that the presence of Cu^{2+} , Pb^{2+} , and Zn^{2+} could not form secondary metal-bearing minerals, but those metal ions may be sitting on the struvite surface.

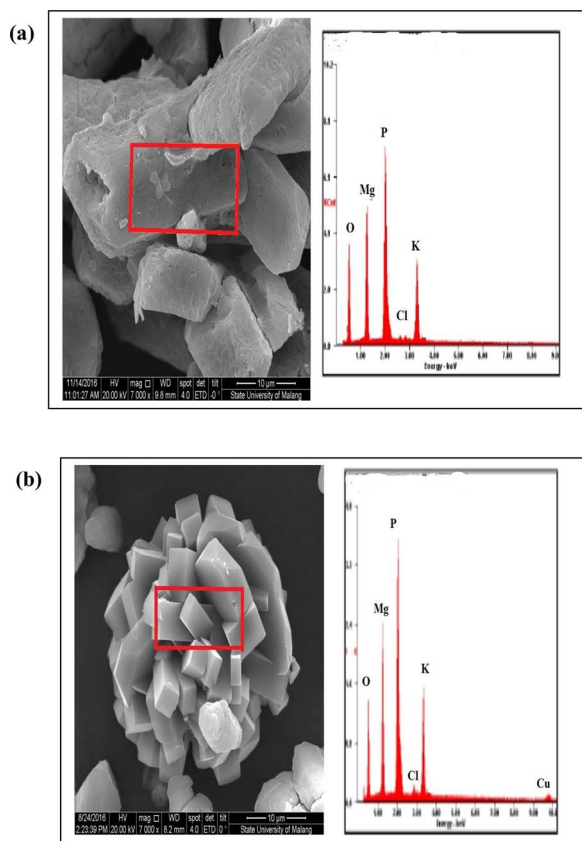


Fig. 5. SEM image and EDX spectrum obtained from the precipitates in the presence of (a) 0 ppm, (b) 100 ppm Cu^{2+} .

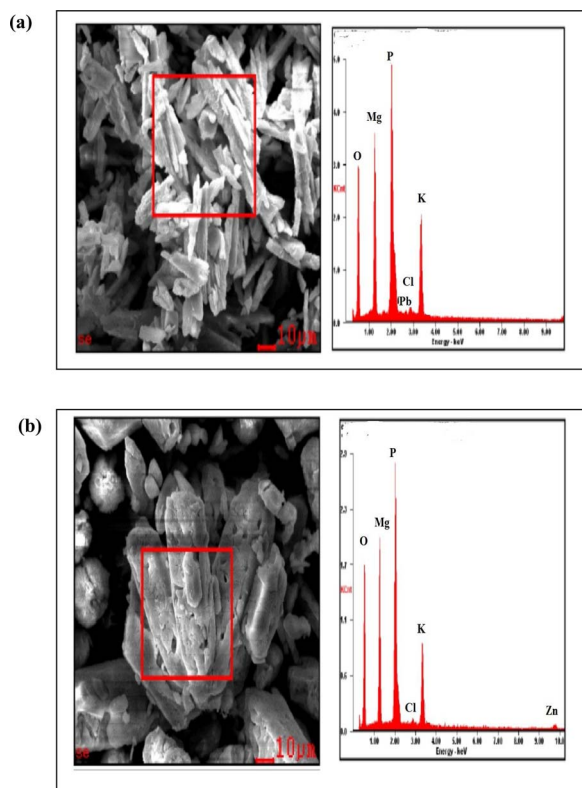


Fig. 6. SEM image and EDX spectrum obtained from the precipitates in the presence of (a) 100 ppm Pb^{2+} ; (b) 100 ppm Zn^{2+} .

Table 7
XRPD-based mineralogy of the precipitates in the presence of metal ions.

Mineral (wt.%)	0 ppm	1 ppm	10 ppm	50 ppm	100 ppm
Cu					
Struvite	99.2	98.9	98.9	98.5	99.5
Sylvite	0.8	1.1	1.1	1.5	0.5
Pb					
Struvite	99.2	99.2	99.6	99.5	99.4
Sylvite	0.8	0.8	0.4	0.5	0.6
Zn					
Struvite	99.2	99.2	99.4	99.2	99.8
Sylvite	0.8	0.8	0.6	0.8	0.2

3.5. Significant finding of the study

The results have demonstrated the precipitation strategy, providing a significant proportion of struvite to recover phosphate and metal ions of Cu^{2+} , Pb^{2+} , and Zn^{2+} from the wastewater, in addition to the minor impurity of sylvite. In the precipitation process, two different stages: nucleation and crystal growth could be observed in the pH measured over time. In the absence of metal ions, nucleation and subsequently struvite crystal growth of the existing nucleation sites is primarily controlled by the mixing speed. The mixing speed (200 rpm) used in this study may have a significant effect on the formation of high purity of struvite [32,33]. The rate of struvite precipitation in the absence of metal ion is very fast in less than 10 min for the first step and then precipitation rate slower in the second step for completing in 70 min under the conditions studied. In contrast, the crystallization times and the precipitation rates observed were affected significantly by the concentrations of metal ions (1–100 ppm). The rates of precipitation in the presence of metals were in all cases lower than those of the absence of metal. Correspondingly the increase in concentrations of metal ions could promote the decreasing absorption rates of the metals. Here, it was possible to significantly reduce concentrations of metal ions in the solution through struvite precipitation.

Further, the initial pH of the solution is the main experimental condition influencing metal ions in struvite formation. The lower the pH, the greater the heavy metal ions is adsorbed by struvite. The optimum adsorption capacity for Cu^{2+} , Pb^{2+} , and Zn^{2+} was reported to be at pH values between 4 and 6 [34]. The findings of the experiments are shown that the different concentrations of the single metal ion solution had an impact on the absorption rate of metals. However, in the range of pH between 4 and 14, other complexes, such as newberyite and bobierrite, may also be formed and consume ions involved in struvite formation [25]. It is suggested that the prepared crystal forming solution over wide ranges of pH values will be completed to fully understand the complexity of struvite formation in absorbing the metals. Moreover, the metals appear to be preferentially associated with struvite, because no evidence of any phases containing Cu^{2+} , Pb^{2+} , and Zn^{2+} was detected by the XRPD Rietveld method. However, these elements may be sitting on the crystal surface [35]. Work remains to be carried out to investigate the behavior of crystal surface for adsorbing the metals.

An SEM/EDX examination of the precipitating solids indicated that the solids are composed of struvite and sylvite as shown in the EDX spectrum. Through SEM, all the particles precipitated show morphological characteristics of struvite [36]. Other precipitates, e.g. sylvite is not visually detected due to their presence being in trace amounts only.

4. Conclusions

It can be concluded that struvite could be potential absorber with respect to heavy metals in solution. The rate of struvite precipitation reduced in the presence of an increase in the content of ion metals.

Detailed mineralogical analysis has been employed to identify mineralogical phase of the precipitating solid. Struvite is a major mineral controlling MAP ions recovery out of the solution at the temperature of 30 °C and initial pH 6.5. The significant proportion of struvite containing heavy metals was precipitated in the solution. The minor impurity of sylvite was formed in all precipitating solids observed. No specific secondary metal bearing minerals were found in association with heavy metals. The struvite crystal has a prismatic morphology, while there is morphological distortion in the presence of heavy metals on the surface of crystal.

Acknowledgements

The study was supported by Universitas Pembangunan Nasional “Veteran” Jawa Timur, Surabaya, Indonesia under the PhD research grant programs.

References

- [1] A. Korchev, H. Saidou, M.B. Amor, Phosphate recovery through struvite precipitation by CO₂ removal: effect of magnesium, phosphate and ammonium concentrations, *J. Hazard. Mater.* 186 (2011) 602–613.
- [2] A.A. Rouff, Sorption of chromium with struvite during phosphorus recovery, *Environ. Sci. Technol.* 46 (2012) 12493–12501.
- [3] A.A. Rouff, V. Marlon Ramlogan, A. Rabinovich, Synergistic removal of zinc and copper in greenhouse waste effluent by struvite, *ACS Sustain. Chem. Eng.* 4 (2016) 1319–1327.
- [4] H. Huang, D.S. Mavinic, K.V. Lo, F.A. Koch, Production and basic morphology of struvite crystals from a pilot-scale crystallization process, *Environ. Technol.* 27 (2006) 233–245.
- [5] H. Huang, P. Zhang, L. Yang, D. Zhang, G. Guo, J. Liu, A pilot-scale investigation on the recovery of zinc and phosphate from phosphating wastewater by step precipitation and crystallization, *Chem. Eng. J.* 317 (2017) 640–650.
- [6] M.A. Barakat, Review Article New trends in removing heavy metals from industrial wastewater, *Arab. J. Chem.* 4 (2011) 361–377.
- [7] F. Ge, M.-M. Li, H. Ye, B.-X. Zhao, Effective removal of heavy metal ions Cd²⁺, Zn²⁺, Pb²⁺, Cu²⁺ from aqueous solution by polymer-modified magnetic nanoparticles, *J. Hazard. Mater.* 211–212 (2012) 366–372.
- [8] A. Aklil, M. Mouflih, S. Sebti, Removal of heavy metal ions from water by using calcined phosphate as a new adsorbent, *J. Hazard. Mater.* A 112 (2004) 183–190.
- [9] Y.F. Lin, H.W. Chen, P.S. Chien, C.S. Chiou, Application of bifunctional magnetic adsorbent to adsorb metal cations and anionic dyes in aqueous solution, *J. Hazard. Mater.* 185 (2011) 1124–1130.
- [10] R. Yu, H. Ren, Y. Wang, L. Ding, J. Geng, K. Xu, Y. Zhang, A kinetic study of struvite precipitation recycling technology with NaOH/Mg(OH)₂ addition, *Bioresour. Technol.* 143 (2013) 519–524.
- [11] M. Ronteltapa, M. Maurera, W. Gujera, The behaviour of pharmaceuticals and heavy metals during struvite precipitation in urine, *Water Res.* 41 (2007) 1859–1868.
- [12] A. Uysal, Y.D. Yilmazel, G.N. Demirel, The determination of fertilizer quality of the formed struvite from effluent of a sewage sludge anaerobic digester, *J. Hazard. Mater.* 181 (2010) 248–254.
- [13] S. Muryanto, A.P. Bayuseno, Influence of Cu²⁺ and Zn²⁺ as additives on precipitation kinetics and morphology of struvite, *Powder Technol.* 253 (2014) 602–607.
- [14] E. Pehvilan, T. Altun, S. Parlayici, Utilization of barley straws as biosorbents for Cu²⁺ and Pb²⁺ ions, *J. Hazard. Mater.* 164 (2009) 982–986.
- [15] T. Zehra, L.B.L. Lim, N. Priyantha, Characterization of peat samples collected from Brunei Darussalam and their evaluation as potential adsorbents for Cu (II) removal from aqueous solution, *Desalin. Water Treat.* (2015) 1–15.
- [16] M. Ajmal, R. Ali Khan Rau, R. Ahmad, Adsorption studies of heavy metals on tectona grandis: removal and recovery of Zn (II) from electroplating wastes, *J. Dispers. Sci. Technol.* 32 (2011) 851–856.
- [17] S.I. Lee, S.Y. Weon, C.W. Lee, B. Koopman, Removal of nitrogen and phosphate from wastewater by addition of bittern, *Chemosphere* 51 (2003) 265–271.
- [18] J.D. Doyle, S.A. Parsons, Struvite formation. control and recovery, *Water Res.* 36 (2002) 3925–3940.
- [19] USEPA, A Geochemical Assessment Model for Environmental Systems: Version 3.0 User Manual, U.S.EPA.EPA/600/3-91/021, Washington, DC, 1991.
- [20] H.M. Rietveld, A profile refinement method for nuclear and magnetic structures, *J. Appl. Crystallogr.* 2 (1969) 65–71.
- [21] J. Rodriguez-Carvajal, Program Fullprof 2k, Version 3.30, Laboratoire Leon Brillouin, France, 2005 June.
- [22] G. Caglioti, A. Paoletti, F.P. Ricci, Choice of collimator for a crystal spectrometer for neutron diffraction, *Nucl. Instrum.* 35 (1958) 223–228.
- [23] A.P. Bayuseno, W.W. Schmahl, Improved understanding of the pozzolanic behaviour of MSWI fly ash with Ca(OH)₂ solution, *Int. J. Environ. Waste Manage.* 15 (2015) 39–66.
- [24] M.S. Rahaman, D.S. Mavinic, N. Ellis, Effects of various process parameters on struvite precipitation kinetics and subsequent determination of rate constants, *Water Sci. Technol.* 57 (2008) 647–654.
- [25] I. Ali, P. Schneider, An approach of estimating struvite growth kinetic incorporating thermodynamic and solution chemistry, kinetic and process description, *Chem. Eng. Sci.* 63 (2008) 3514–3525.
- [26] N.O. Nelson, R.L. Mikkelsen, D.L. Hesterberg, Struvite precipitation in anaerobic swine lagoon liquid: effect of pH and Mg: P ratio and determination of rate constant, *Bioresour. Technol.* 89 (2003) 229–236.
- [27] K.N. Ohlinger, T.M. Young, E.D. Schroeder, Postdigestion struvite precipitation using a fluidized bed reactor, *J. Environ. Eng.* 126 (2000) 361–368.
- [28] T.A. Hoang, H.M. Ang, A.L. Rohl, Effects of organic additives on calcium sulfate scaling in pipes, *Aust. J. Chem.* 62 (2009) 927–933.
- [29] A. Whitaker, J.W. Jeffery, The crystal structure of struvite, MgNH₄PO₄·6H₂O, *Acta Crystallogr.* B26 (1970) 1429–1440.
- [30] H. Ott, Die Strukturen von Mn O, Mn S Ag F, Ni S, Sn I4, Sr Cl₂, Ba F₂, praezisionsmessungen einiger alkalihalogenide, *Z. Kristallogr.* 63 (1926) 222–230.
- [31] D.S. Perwitasari, L. Edahwati, S. Sutiyono, S. Muryanto, J. Jamari, A.P. Bayuseno, Phosphate recovery through struvite-family crystals precipitated in the presence of citric acid: mineralogical phase and morphology evaluation, *Environ. Technol.* 38 (22) (2017) 2844–2855.
- [32] A. Capdeviellea, E. Sykorová, B. Biscans, F. Bélinea, M.-L. Daumer, Optimization of struvite precipitation in synthetic biologically treated swine wastewater-Determination of the optimal process parameters, *J. Hazard. Mater.* 244–245 (244) (2013) 357–.
- [33] C.M. Mehta, D.J. Batstone, Nucleation and growth kinetics of struvite precipitation, *Water Res.* 47 (2013) 2890–2900.
- [34] C. Peng, L.-Y. Chai, C.-J. Tang, X.-B. Min, M. Ali, Y.-X. Song, W.-M. Qi, Feasibility and enhancement of copper and ammonia removal from wastewater using struvite formation: a comparative research, *J. Chem. Technol. Biotechnol.* 92 (2017) 325–333.
- [35] A.P. Bayuseno, W.W. Schmahl, Th. Müllejjans, Hydrothermal processing of MSWI fly Ash-towards new stable minerals and fixation of heavy metals, *J. Hazard. Mater.* 167 (2009) 250–259.
- [36] W. Tao, K.P. Fattah, M.P. Huchsermeier, Struvite recovery from anaerobically digested dairy manure: a review of application potential and hindrances, *J. Environ. Manage.* 169 (2016) 46–57.